

## References

- ZIRNGIBL, M., DRAGONE, C., and JOYNER, C.H.: 'Demonstration of a  $15 \times 15$  arrayed waveguide multiplexer on InP', *IEEE Photonics Technol. Lett.*, 1992, 4, (11), pp. 1250–1253
- VERBEEK, B.H., STARING, A.A.M., JANSEN, E.J., VAN-ROUEN, R., BINSMA, J.J.M., VAN-DONGEN, T., AMERSFOORT, M.R., VAN-DAM, C., and SMIT, M.K.: 'Large bandwidth polarisation independent and compact eight channel PHASAR demultiplexer/filter'. OFC '94, San Jose, 20–25 February 1994, Paper PD13-1
- BISSESSUR, H., MARTIN, B., MESTRIC, R., and GABORIT, F.: 'Small-size polarisation-independent phased array demultiplexers on InP', *Electron. Lett.*, 1995, 31, (24), pp. 2118–2119
- BISSESSUR, H., GABORIT, E., MARTIN, B., and RIPOCHE, G.: 'Polarisation-independent phased-array demultiplexer on InP with high fabrication tolerance', *Electron. Lett.*, 1995, 31, (16), pp. 1372–1373
- BISSESSUR, H., PAGNOD-ROSSIAUX, M., MESTRIC, R., and MARTIN, B.: 'Extremely small polarization independent phased-array demultiplexers on InP', *IEEE Photonics Technol. Lett.*, 1996, 8, (4), pp. 554–556
- ZIRNGIBL, M., JOYNER, C.H., STULZ, L.W., GAIFFE, T.H., and DRAGONE, C.: 'Polarisation independent  $8 \times 8$  waveguide grating multiplexer on InP', *Electron. Lett.*, 1993, 29, (2), pp. 201–202
- ZIRNGIBL, M., JOYNER, C.H., and CHOU, P.C.: 'Polarisation compensated waveguide grating router on InP', *Electron. Lett.*, 1995, 31, (19), pp. 1662–1663
- SOOLE, J.B.D., AMERSFOORT, M.R., LEBLANC, H.P., ANDREADAKIS, N.C., RAJHEL, A., CANEAU, C., KOZA, M.A., BHAT, R., YOUTSEY, C., and ADESIDA, I.: 'Polarisation-independent InP arrayed waveguide filter using square cross-section waveguides', *Electron. Lett.*, 1996, 32, (4), pp. 323–324
- ZIRNGIBL, M., JOYNER, C.H., STULZ, L.W., KOREN, U., CHIEN, M.-D., YOUNG, M.G., and MILLER, B.I.: 'Digitally tunable laser based on the integration of a waveguide grating multiplexer and an optical amplifier', *IEEE Photonics Technol. Lett.*, 1994, 6, (4), pp. 516–518
- JOYNER, C.H., ZIRNGIBL, M., and MEESTER, J.P.: 'A multifrequency waveguide grating laser by selective area epitaxy', *IEEE Photonics Technol. Lett.*, 1994, 6, (11), pp. 1277–1279

## Table-based log-domain linear transformation filter

Shen Iuan Liu and Yu-Hung Liao

*Indexing terms:* Active filters, Ladder filters, Elliptic filters

A design table for realising log-domain linear transformation filters is presented. Based on this design table, doubly terminated LC ladder filters with or without finite transmission zeros can be efficiently synthesised. Moreover, two design procedures are also given. A canonical log-domain elliptic ladder filter can be realised using one of these procedures. Simulation results are given to verify the theoretical analysis.

**Introduction:** Log-domain filters [1–3] have been receiving significant attention in current-mode analogue filters. However, the synthesis method [1] based on the state equations for realising high-order LC ladder filters is complicated. A signal-flow-graph-based method [3] has been presented to synthesise high-order LC ladder filters, but it can only synthesise all-pole filters. In this Letter, a log-domain linear transformation method has been developed to realise the doubly terminated LC ladder filters with or without transmission zeros. A design table is presented and two synthesis procedures have also been developed. Simulation results are given to verify theoretical analysis.

**Circuit description:** Using the linear transformation method [4], we can transform the input and output voltage and current variables of a two-port network into two new variables  $x_i$  and  $y_i$ . Their characteristics can be described by the following matrix:

$$\begin{bmatrix} x_i \\ y_i \end{bmatrix} = \begin{bmatrix} \alpha_i & \beta_i \\ \gamma_i & \delta_i \end{bmatrix} \begin{bmatrix} V_i \\ I_i \end{bmatrix} \quad i = 1 \text{ and } 2 \quad (1)$$

where  $x_i$  and  $y_i$  have the dimensions of voltages, e.g. the series section of an LC ladder filter with a floating capacitor in parallel

with a floating inductor is shown in the last row of Fig. 3. If we choose the transformation matrices as

$$\begin{bmatrix} \alpha_1 & \beta_1 \\ \gamma_1 & \delta_1 \end{bmatrix} = \begin{bmatrix} 1 & 0 \\ 0 & R \end{bmatrix} \quad \text{and} \quad \begin{bmatrix} \alpha_2 & \beta_2 \\ \gamma_2 & \delta_2 \end{bmatrix} = \begin{bmatrix} 1 & 0 \\ 0 & -R \end{bmatrix} \quad (2)$$

The new variables,  $x_1$ ,  $y_1$ ,  $x_2$  and  $y_2$  can be obtained and expressed as

$$y_1 = y_2 = \frac{s^2 LC + 1}{sL/R} (x_1 - x_2) \quad (3)$$

Using the translinear principle of bipolar transistors [1, 3], the corresponding log-domain circuit is shown in Fig. 3 with the design equations

$$\frac{2V_T}{I_0} C_L = \frac{L}{R} \quad \text{and} \quad \frac{2V_T}{I_0} C_C = RC \quad (4)$$

where  $V_T$  is the thermal voltage and  $I_0$  is a DC current source. Similarly, the corresponding input and output termination sections, and the series and shunt sections, can also be established, and they are listed in Fig. 3. To avoid the complexity of general interconnection between the new two-port networks, the cross-cascade interconnection [4–6] is introduced. From this cross-cascade interconnection, the new port variables  $x_1$  and  $x_2$  of the floating LC section, which are exactly equal to the original port voltages  $V_1$  and  $V_2$ , respectively, can be found [6]. Moreover, the corresponding voltage variables in the log-domain will be also equal, respectively. Thus, an alternative method can be used to synthesise the parallel LC series section. First, we can separate the floating capacitor from the floating LC section and synthesise it as the floating inductor. Then, the floating capacitor is inserted into the corresponding nodes.

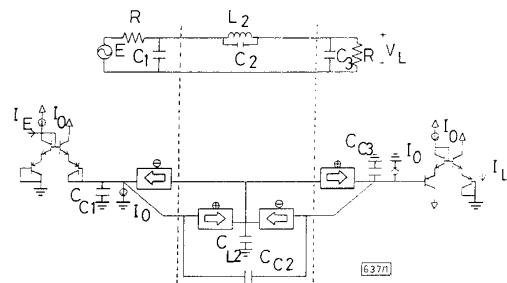


Fig. 1 Typical design example of a log-domain third-order elliptic filter

If only grounded capacitors are available, the design procedure for the elliptic LC ladder filter can be: first, divide the original ladder prototype into several sections and choose the corresponding log-domain counterparts, then connect these circuits with a cross-cascade interconnection [4]. Finally, determine the values of currents  $I_0$  and capacitors. The advantage of this method is that it only requires grounded capacitors [7]. If floating capacitors are available, we can separate them from the original prototype and synthesise the all-pole filter alone. Finally, insert the floating capacitors into their corresponding nodes to complete the synthesis of the elliptic filters. This approach is suitable for high frequency operation, because all nodes have a desired capacitance and the parasitic capacitances can be included in the circuit capacitances [8].

**Simulation results:** A prototype third-order elliptic ladder filter with 0.15dB ripple is shown in Fig. 1. First, we can separate the floating capacitor  $C_2$  from the original prototype and divide it into three sections. Next, connect the corresponding log-domain circuits in Fig. 1 with a cross-cascade interconnection. Finally, insert the floating capacitor  $C_2$  into the corresponding nodes. The resulting synthesised log-domain filter is shown in Fig. 1. The power supply voltages are  $\sim 5V$  and the DC current sources  $I_0 = 200\mu A$ . The parameters of the npn ( $\beta_{npn} = 160$ ) and pnp ( $\beta_{pnp} = 55$ ) bipolar transistors are adapted from a standard  $2\mu m$  BiCMOS process [9]. The values of the capacitors are  $C_{C1} = C_{C3} = 0.9079nF$ ,  $C_{C2} = 0.0846nF$  and  $C_{L2} = 1.0531nF$ . The comparisons between the simulation and theoretical results are shown in Fig. 2. The simulation results have 0.75dB loss in the passband compared with the theoretical analysis.

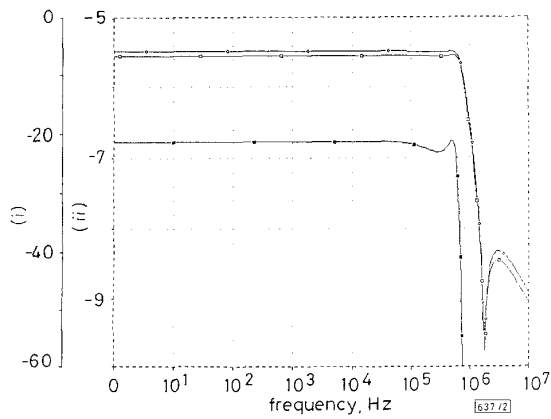


Fig. 2 Comparisons between simulation and theoretical results of Fig. 1

- (i)  $\square$  simulated  
 (ii)  $\blacklozenge$  theoretical  
 (ii) expanded view of passband of proposed filter

Filter section	Transformation matrix and transfer function	corresponding log-domain circuit and design equation
	$\begin{bmatrix} 0 & -R \\ 1 & 0 \end{bmatrix}$ $y_2 = \frac{E - X_2}{sRC + 1}$	
	$\begin{bmatrix} 1 & 0 \\ 0 & -R \end{bmatrix}$ $y_2 = \frac{E - X_2}{sL/R + 1}$	
	$\begin{bmatrix} 0 & R \\ 1 & 0 \end{bmatrix}$ $y_1 = \frac{X_1}{sRC + 1}$	
	$\begin{bmatrix} 1 & 0 \\ 0 & R \end{bmatrix}$ $y_1 = \frac{X_1}{sL/R + 1}$	
	$\begin{bmatrix} 0 & R \\ 1 & 0 \end{bmatrix}$ $\begin{bmatrix} 0 & -R \\ 1 & 0 \end{bmatrix}$ $y_1 = y_2 = \frac{X_1 - X_2}{sRC}$	
	$\begin{bmatrix} 1 & 0 \\ 0 & R \end{bmatrix}$ $\begin{bmatrix} 1 & 0 \\ 0 & -R \end{bmatrix}$ $y_1 = y_2 = \frac{X_1 - X_2}{sL/R}$	
	$\begin{bmatrix} 0 & R \\ 1 & 0 \end{bmatrix}$ $\begin{bmatrix} 0 & -R \\ 1 & 0 \end{bmatrix}$ $y_1 = y_2 = \frac{(s^2LC + 1)(X_1 - X_2)}{sRC}$	
	$\begin{bmatrix} 1 & 0 \\ 0 & R \end{bmatrix}$ $\begin{bmatrix} 1 & 0 \\ 0 & -R \end{bmatrix}$ $y_1 = y_2 = \frac{(s^2LC + 1)(X_1 - X_2)}{sL/R}$	

Fig. 3 Design table for ladder filters with or without transmission zeros

**Conclusions:** An efficient design table has been established, and a third-order elliptic ladder filter has been synthesised. Simulation results have also been given to verify the theoretical analysis. The proposed method is expected to be useful in the synthesis of log-domain ladder filters with or without transmission zeros.

© IEE 1996

12 June 1996

Electronics Letters Online No: 19961181

Shen Iuan Liu and Yu-Hung Liao (Department of Electrical Engineering, National Taiwan University, Taipei, Taiwan 10664, Republic of China)

## References

- 1 FREY, D.: 'Log domain filtering: An approach to current mode filtering', *IEEE Proc. Devices, Circuits Syst.*, 1993, **140**, pp. 406-416

- 2 TOUMAZOU, C., NGARMNIL, J., and LANDE, T.S.: 'Micropower log-domain filter for electronic cochlea', *Electron. Lett.*, 1994, **30**, pp. 1839-1841
- 3 PERRY, D., and ROBERTS, G.W.: 'Log-domain filters based on LC ladder synthesis'. *IEEE Int. Symp. Circuits Syst.*, 1995, pp. 311-314
- 4 DIMOPOULOS, H.G., and CONSTANTINIDES, A.G.: 'Linear transformation active filters', *IEEE Trans. Circuits Syst.*, 1978, **CAS-25**, pp. 845-852
- 5 HWANG, Y.S., LIU, S.I., WU, D.S., and WU, Y.P.: 'Table-based linear transformation filters using OTA-C Techniques', *Electron. Lett.*, 1994, **30**, pp. 2021-2022
- 6 HWANG, Y.S., CHIU, W., LIU, S.I., WU, D.S., and WU, Y.P.: 'High-frequency linear transformation elliptic filters employing minimum number of OTAs', *Electron. Lett.*, 1995, **31**, pp. 1562-1564
- 7 BHUSAN, M., and NEWCOMB, R.W.: 'Grounding of capacitors in integrated circuits', *Electron. Lett.*, 1967, **3**, pp. 148-149
- 8 NAUTA, B.: 'Analog CMOS filters for very high frequencies' (Kluwer Academic Publishers, 1993)
- 9 ISMAIL, M., and FIEZ, T.: 'Analog VLSI signal and information processing' (McGraw-Hill, 1994)

## Fuzzy pattern spectrum as a texture descriptor

M. Ghadiali, J.C.H. Poon and W.C. Siu

*Indexing terms:* Texture (image processing), Fuzzy systems

The authors introduce a novel descriptor for texture classification, namely the fuzzy pattern spectrum (FPS). Essentially, the FPS is a novel extension of the traditional morphological pattern spectrum, the significant advantage being its effectiveness in quantifying spatial uncertainty in images. A texture classification experiment is discussed to show the usefulness of the FPS wherein a classification accuracy of 94% is achieved.

**Introduction:** Mathematical morphology is a powerful tool for shape and feature analysis and feature representation. Work [1] in this field has sought to augment the scope of traditional morphology using the tools of fuzzy sets, hence gaining an understanding of the 'spatial uncertainty' or 'fuzziness' in image features. Fuzzy mathematical morphology extends the intuitive notion of 'fitting' in traditional morphology, to the 'degree of fitting'.

In fuzzy mathematical morphology, the degree of subthreshold between the image and the structuring element needs to be determined. This is realised using an indicator function which is essentially a mapping from two fuzzy sets, the image A and structuring element B, to another fuzzy set (the degree of set inclusion). Based on this, the representation for fuzzy erosion [2],  $\mu_{E(A,B)}(x)$ , is as follows:

$$\mu_{E(A,B)}(x) = \inf \min[1, 1 + \mu_A(x) - \mu_B(x)] \quad (1)$$

$\mu_A(x)$  and  $\mu_B(x)$  denote memberships of element x to the fuzzy sets A and B, respectively.

**Texture classification using FPS:** Multi-scaled morphological operations have been used to generate shape-size descriptors termed the pattern spectrum [3] or the pectrum [4]. The pattern spectrum can be considered to be analogous to the Fourier spectrum, the difference being that the first quantifies shape, whereas the latter quantifies the frequency distribution of the signal. Morphological operations are used to generate descriptors that determine up to what scale a given shape exists in an image. A structuring element B can generate a multi-scale family of structuring elements by dilating itself, thus:

$$nB = B \oplus B \oplus B \cdots \oplus B \quad (n \text{ times}) \quad n = 0, 1, 2, \dots \quad (2)$$

A family of multi-scale erosions where B is the generator is denoted by

$$X^{En} = [(X \ominus nB)] \quad (3)$$

where  $X^{En}$  represents the erosion of image X by nB.